Composite Structures 120 (2015) 79–89

Contents lists available at ScienceDirect

Composite Structures

journal homepage: www.elsevier.com/locate/compstruct

Localization of buckling modes in plates and laminates

S. Paik [a], S.S. Gupta [a,*], R.C. Batra [b]

[a] Mechanics and Applied Mathematics Group, Department of Mechanical Engineering, Indian Institute of Technology-Kanpur, Kanpur 208016, India
[b] Department of Biomedical Engineering and Mechanics, M/C 0219, Virginia Polytechnic Institute and State University, Blacksburg, VA 24061, USA

ARTICLE INFO

Article history:
Available online 30 September 2014
This paper is dedicated to the memory of the late Professor Himanshu Hatwal, Department of Mechanical Engineering, IIT Kanpur, India.

Keywords:
Mindlin plate theory
Buckling
Laminates
Mode localization

ABSTRACT

We use the Mindlin plate theory and the finite element method to delineate the effect of fixing points on a transverse normal to the mid-surface of the plate on the localization of buckling modes in clamped–clamped rectangular plates made of linear elastic, homogeneous and either isotropic (monolithic) or orthotropic (fiber-reinforced composite) materials. The in-plane loads considered on the bounding edges are: (i) normal tractions on the length, (ii) normal tractions on the width, (iii) equal normal tractions on the length and the width (equal biaxial loading), (iv) shear (tangential), and (v) combined same normal and shear tractions on all sides. It is found that clamping points on a transverse normal passing through the mid-point of a line parallel to the short side increases the critical buckling load of plates of only low aspect ratios over that of the corresponding plates unconstrained at interior points. However, for plates of all aspect ratios (thickness/length) fixing points on a transverse normal divides it into two regions with negligible transverse deflections in only one of the two regions. Only for loads (i)–(iii) the dividing line is parallel to the short side of the plate. For both thin and thick isotropic plates the slope of the dividing line is found to monotonically increase with an increase in the aspect ratio of a plate until it reaches a saturation value. A parameter based on the modal strain energy is used to quantify the degree of localization of a buckling mode. For an isotropic plate the degree of localization is found to increase with the increase in the aspect ratio for load cases (i)–(iii) but is found to be moderate for load cases (iv) and (v). For an orthotropic layer the degree of localization with an increase in the aspect ratio of the plate increases more for the 90° lamina than that for the 0° and the 45° laminae. Also, the mode localization in the (45°, −45°) laminate is stronger than that in the (0°, 90°) laminate for the five load cases. However, moderate degree of mode localization is found in symmetric and anti-symmetric cross-ply and angle-ply laminates.

1. Introduction

An irregularity in an ordered medium generally leads to localization of vibration modes [1,2] in linear mechanical systems, i.e., the vibration modes are confined in a certain region of the system. Since a buckling problem is also an eigenvalue problem it may be envisaged that a disturbance in the periodic order in a mechanical system will lead to buckling mode localization [3]. Pierre and Plaut [3] considered a beam made of two spans of identical uniform cross-sections but of different lengths, fixed at one end while supported on rollers at the intermediate point and at the other end, with the two spans coupled with a torsional spring. For the beam loaded by an axial compressive force, they used perturbation analysis and found mode localization for weak coupling between the two spans. They concluded that the loci of the first two critical loads as a function of the slight irregular spacing between the two supports are far separated for strong coupling and are very close to each other for weak coupling between the spans. Similarly, Nayfeh and Hawwa [4] studied localization of buckling modes in three and four span simply supported beams coupled through torsional springs, and Li et al. [5] extended this work to an *N*-span beam. By using Kirchhoff's plate theory Elishakoff et al. [6] found that the buckling mode localization is sensitive to the misplacement of stiffeners in uniaxially compressed rib-stiffened rectangular thin plates. These plates with different boundary conditions were subsequently analyzed by Xie and Ibrahim [7] using the finite strip method. Xie [8] found that a stronger inhomogeneity leads to a larger degree of buckling mode localization in a simply-supported nonhomogeneous beam resting on an elastic foundation and loaded by in-plane compressive loads. Brasil and Hawwa [9] studied buckling mode localization in two-dimensional trusses by slightly varying the length of a truss member.

Filoche and Mayboroda [10] have studied vibration mode localization in a linear elastic, isotropic and homogeneous Kirchhoff plate, and showed that fixing points on a transverse normal divides

* Corresponding author.
E-mail address: ssgupta@iitk.ac.in (S.S. Gupta).

http://dx.doi.org/10.1016/j.compstruct.2014.09.035
0263-8223/

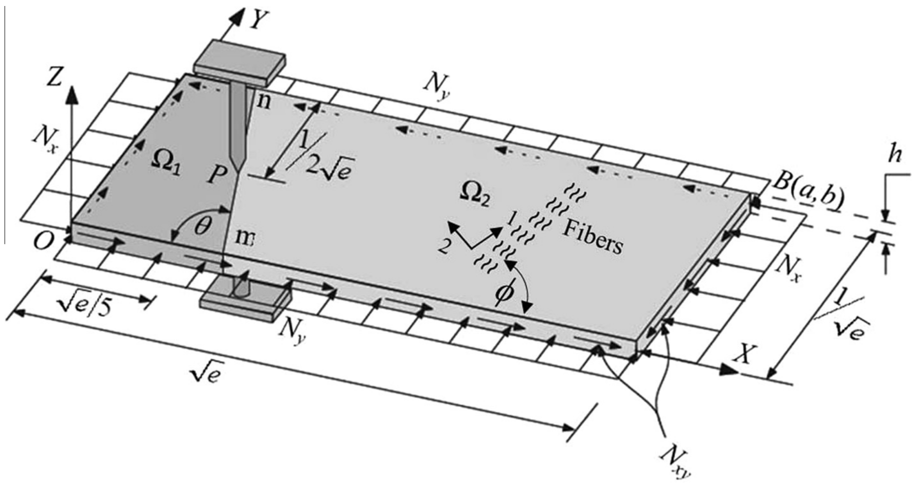

Fig. 1. Schematic of a clamped–clamped plate depicting geometric parameters, orientation of fibers and fiber axis for laminae/laminates, the location of the interior point P on the plate mid-surface, different uniformly distributed loads on the edge surfaces, and regions Ω_1 (shaded) and Ω_2 where buckling modes get localized after fixing points on the vertical line passing through the point P. A possible way of fixing points on the vertical line passing through P is shown using two pins supporting the plate from opposite sides, while the other end of pins is fixed. For an isotropic plate the angle θ of the dividing line mn passing through P equals $\pi/2$ for loading scenarios (i)–(iii), and it equals the inclination of the tangent to nodal line $w(x,y) = 0$ through P for the loading situations (iv) and (v).

Table 1
Nondimensional critical buckling load factor k $(= N_0 b^2/\pi^2 D$, where N_0 = the critical buckling load/length, b = width of the plate, and D = bending rigidity of the plate) for CCCC rectangular isotropic plates of b/h = 100 subjected to loads (i) and (iii). Poisson's ratio ν = 0.3.

Eccentricity	Load type (i) (uniaxial compression)		Load type (iii) (shear tractions)	
	Timoshenko and Gere [14]	Present	Shufrin and Eisenberger [15]	Present
0.75	11.69	11.63	–	–
1.00	10.07	10.05	14.64	14.57
1.25	9.25	9.23	–	–
1.50	8.33	8.32	–	–
1.75	8.11	8.09	–	–
2.00	7.88	7.85	10.25	10.21
2.25	7.63	7.61	–	–
2.50	7.57	7.56	–	–
2.75	7.44	7.42	–	–
3.00	7.37	7.34	9.53	9.50
3.25	7.35	7.32	–	–
3.50	7.27	7.24	–	–
3.75	7.24	7.21	–	–
4.00	7.23	7.19	9.30	9.27
6.00	–	–	9.12	9.09
10.00	–	–	9.03	9.00

the plate into two independently vibrating regions. Subsequently, Sharma et al. [11] used the Mindlin plate theory to delineate effects of the fiber angle and the stacking sequence on mode localization, and found that placing a lumped mass at an interior point of a laminate also localized modes of vibration. Verma et al. [12] used molecular mechanics simulations with the MM3 potential and the software TINKER to analyze vibration mode localization in a single- and multi- layered graphene nanoribbon due to either fixing an atom or attaching a buckyball to an atom in the interior of the nanoribbon. Here we use the Mindlin plate theory to study buckling mode localization in clamped–clamped (i) linear elastic, homogeneous and isotropic thin rectangular plates, and (ii) orthotropic laminae and laminates due to fixing points on a transverse normal passing through an interior point P. The following five in-plane loads on the plate edges are considered: (i) normal to the long side, (ii) normal to the short side, (iii) normal to all sides (equal biaxial loading), (iv) shear or tangential on all sides, and (v) combined biaxial and tangential tractions of the same magnitude. For all load types considered, the interior point is found to divide a plate/laminate into two distinct regions – one with buckling mode of finite amplitude and the other of negligible amplitude. We define the degree of mode localization as the ratio of the modal strain energies of one such region to that of the entire plate/laminate. It is found that the degree of mode localization for isotropic monolithic plates increases with an increase in the aspect ratio of plates. For an orthotropic laminae the degree of mode localization is higher for a 90° lamina than that for 0° and 45° laminae for the same relative location of the fixed point. However, there is no appreciable mode localization in symmetric and anti-symmetric, cross-ply and angle-ply laminates with more than two layers. These results can be used to place internal constraints on panels of aircraft/spacecraft skins and on superstructure/bulkhead of ships.

The rest of the paper is organized as follows. In Section 2 we briefly describe the procedure used to analyze the problem. In Section 3, we discuss the buckling mode localization in isotropic plates due to the five load types, and provide the orientation of the in-plane line passing through the interior fixed point which divides the plate into two independent regions. Buckling mode localization in orthotropic laminae and laminates is discussed in Section 4. Conclusions of this work are summarized in Section 5.

2. Procedure

Static deformations of a clamped rectangular plate/laminate with in-plane applied forces at the edges as shown in Fig. 1 are analyzed by using the Mindlin plate theory and the finite element method (FEM) with 8-node quadrilateral elements. The buckling load of a linear elastic plate is given by the eigenvalue problem

$$[K - \lambda K_G]\{\delta\} = 0. \quad (1)$$

Here, K and K_G are the global stiffness and the global geometric matrices, respectively. The eigenvalue λ and the associated eigenvector $\{\delta\}$ are the buckling load and the associated buckling mode, respectively. Each node of the finite element on the midsurface of the plate has three degrees-of-freedom (DOF), namely, w, the displacement along the Z-axis, ψ_X, the rotation about the X-axis of the transverse normal to the mid-plane, and ψ_Y, the rotation about the Y-axis of the transverse normal to the mid-plane. The plate

Table 2
Nondimensional critical buckling load factor k $(= N_0b^2/\pi^2D)$ for CCCC rectangular isotropic plates with $b/h = 100$ and $\nu = 0.3$ and subjected to combined loads, i.e., $N_x = N_y = N_0$ and $N_{xy} = N_{0xy}$.

N_0/N_{0xy}	Timoshenko and Gere [14]	Present
0.0	14.71	14.57
0.5	7.09	7.38
1.0	4.50	4.63
1.5	3.24	3.30
2.0	2.51	2.54

length equals the inverse of its width, the aspect ratio (length/width) following [10] is termed the eccentricity, and the shear correction factor is assigned the value 5/6. Boundary conditions at the clamped edges and at a clamped interior point are: $w = \psi_X = \psi_Y = 0$. For plates of various eccentricities, the FE mesh was refined until the successive refinement yielded the difference between the loads for the first 100 buckled modes of less than 1%. For the plate/laminate with eccentricity of 20 the FE mesh of 18 uniform elements along the width b and 200 uniform elements along the length a gave the converged solution. The bending and the shear parts of an element stiffness matrix for a thin plate are computed by using the 3×3 and the 2×2 Gauss quadrature rule, respectively. The FE code written in MATLAB [13] has been verified by comparing (e.g., see Tables 1 and 2) computed values of the buckling load factor for different loads applied on edges of an unconstrained monolithic plate with those available in the literature. It is found that the computed values of the buckling load factor agree well with those reported by other researchers. Similarly, the computed non-dimensional buckling load factor ($k = N_xb^2/D_0$) of 62.045 for clamped–clamped [30°/−30°/30°] laminated square plate with $E_1/E_2 = 2.45$, $G_{12}/E_2 = 0.48$, $\nu_{12} = 0.23$, $b/h = 100$, $D_0 = E_1h^3/12(1 - \nu_{12}\nu_{21})$, subjected to load type (i) was found to be close to 61.893 reported by Shrufin et al. [16]. Here various symbols have the usual meaning, and h equals the thickness of the plate. Buckling loads found using this code for other boundary conditions at the plate edges and various loads applied on the edge surfaces were also found to agree well with those reported in the literature. These results are omitted for the sake of brevity. This code is used to study buckling mode localization in rectangular plates/laminates of $b/h = 100\,(50)$ for isotropic (orthotropic) plates when points on the transverse normal through the interior point P, shown in Fig. 1, are fixed. The location of the interior point P is found not to affect the mode localization phenomenon.

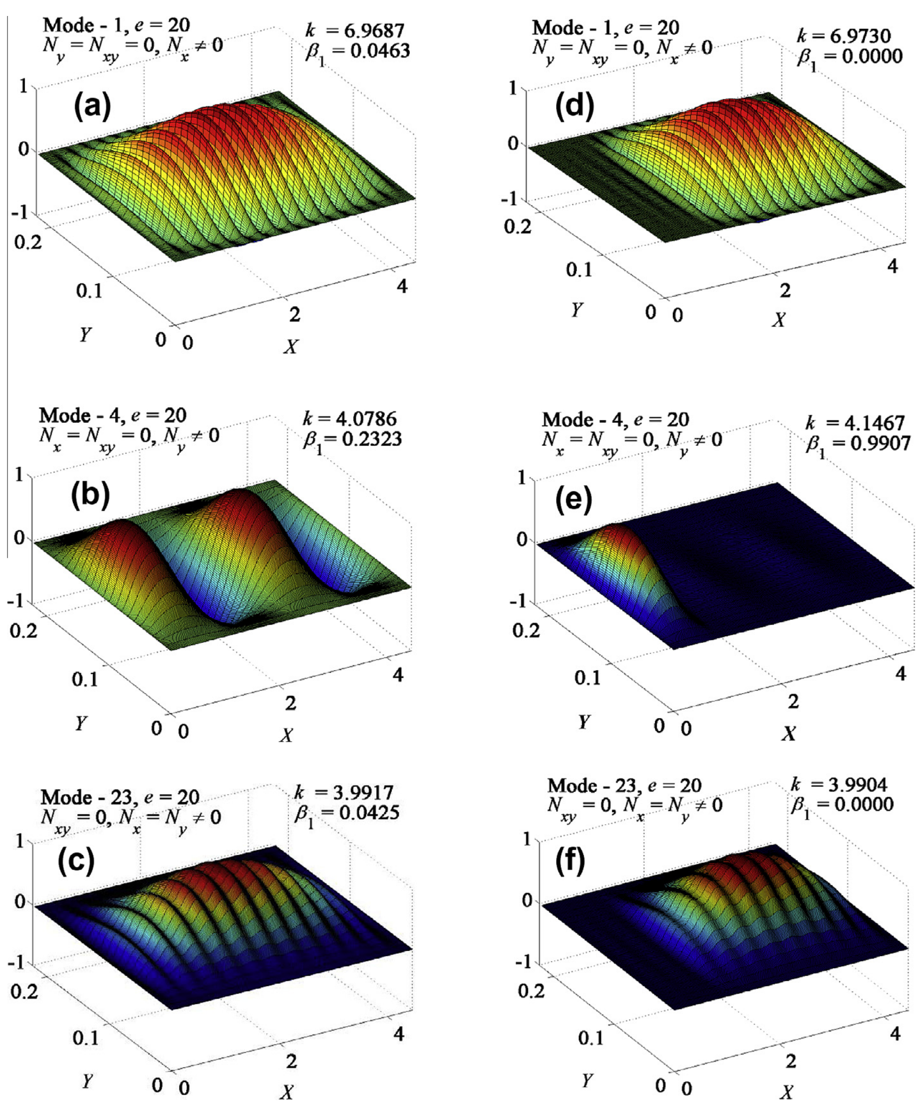

Fig. 2. Normalized buckling modes of the clamped rectangular plate of eccentricity = 20 for different edge loads. Modes in panels (a)–(c) are for the plate with clamped edges, and those in panels (d)–(f) are for the clamped plate when points on the transverse normal through the point P, shown in Fig. 1, are also clamped.

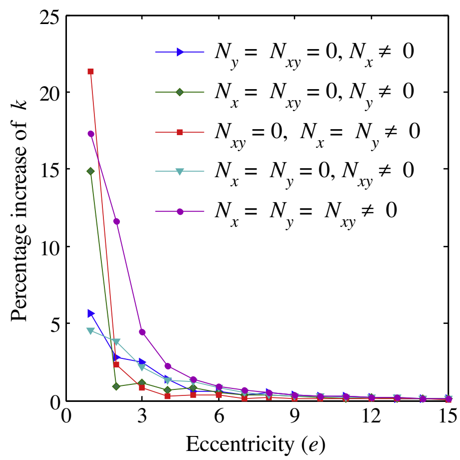

Fig. 3. Effect of clamping points on the transverse normal through the interior point P (as shown in Fig. 1) of an isotropic plate on the critical buckling load with increase in the plate eccentricity. Values along the y-axis are computed with reference to the critical buckling load of an un-constrained clamped plate.

3. Buckling mode localization in isotropic plates

3.1. Loads (i) through (iii)

For an isotropic material we set Young's modulus $E = 10{,}920$ units and Poisson's ratio $\nu = 0.3$. In Fig. 2 we have exhibited buckling mode localization in the plate of eccentricity $e = 20$ for loading scenarios (i) through (iii). It is clearly seen that fixing points on the transverse normal through the interior point P (hereafter referred to as fixing point P) localizes buckling modes on either side of it (cf. Fig. 2d–f). The plate is divided into two regions Ω_1 and Ω_2 by point P (cf. Fig. 1). As shown in Fig. 3, the critical buckling load factor increases after clamping an interior point for each of the three loading cases for plates of aspect ratio < 4. However, with increasing aspect ratio the effect of clamping point P on the critical buckling load diminishes. The critical buckling load is the least for the combined loading.

We quantify buckling mode localization using the energy based non-dimensional parameter β_1, defined by

$$\beta_1 = \frac{\sum_{i=1}^{n}\{\delta\}_i^T[k]_{el}\{\delta\}_i}{\sum_{j=1}^{N}\{\delta\}_j^T[k]_{el}\{\delta\}_j}. \tag{2}$$

That is, β_1 equals the ratio of the modal strain energy of region Ω_1 composed of n elements to that of the modal strain energy of region Ω that is divided into N elements. It should be noted that $\Omega = \Omega_1 \cup \Omega_2$. For an element partially in Ω_1 and Ω_2, the strain energy of deformation of an element attributed to Ω_1 is taken to be proportional to the area of the element in Ω_1. In Eq. (2) $[k]_{el}$ is the stiffness matrix for element el that includes the shear correction factor. Value of $\beta_1 \sim 0$ implies negligible deformations in Ω_1 (cf. Fig. 2d and f) whereas $\beta_1 \sim 1$ implies that deformations are predominantly in Ω_1 (cf. Fig. 2e). The distribution of β_1 for a plate without clamped interior point and subjected to load (i) is shown in Fig. 4a.

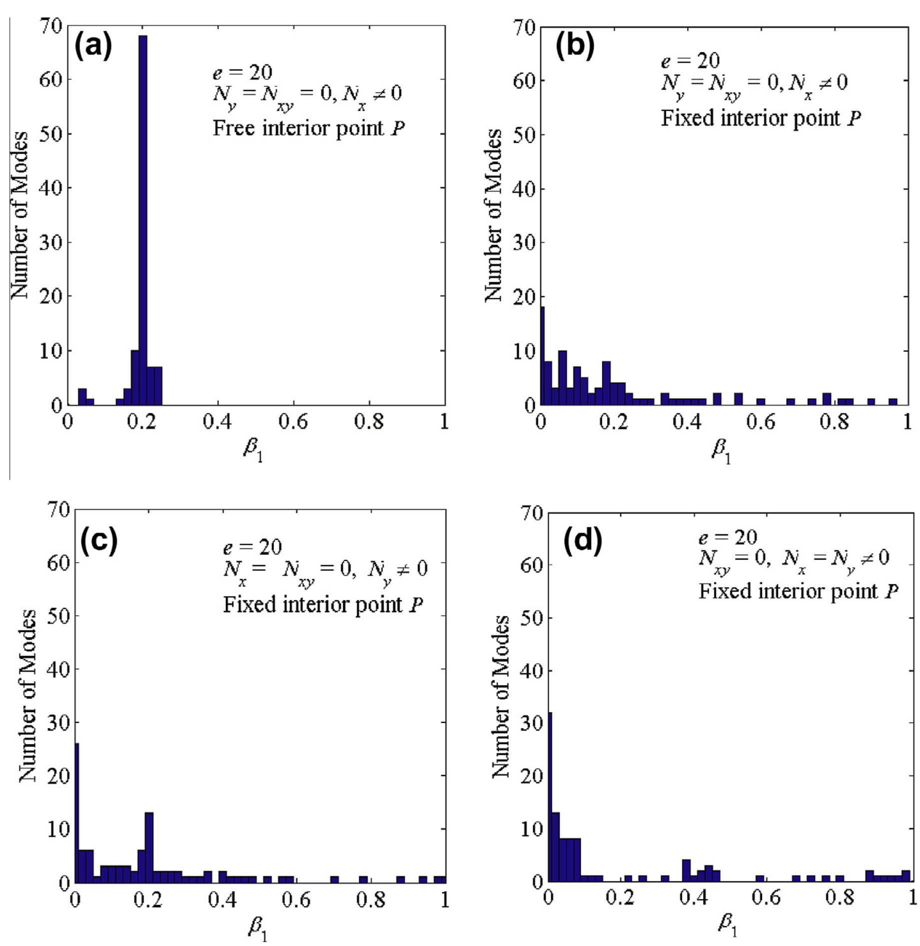

Fig. 4. (a) Distribution of the mode localization parameter β_1 for load case (i) when no interior point is clamped, (b)–(d) distribution of β_1 for the load cases (i), (ii) and (iii) with points on the transverse normal through point P clamped.

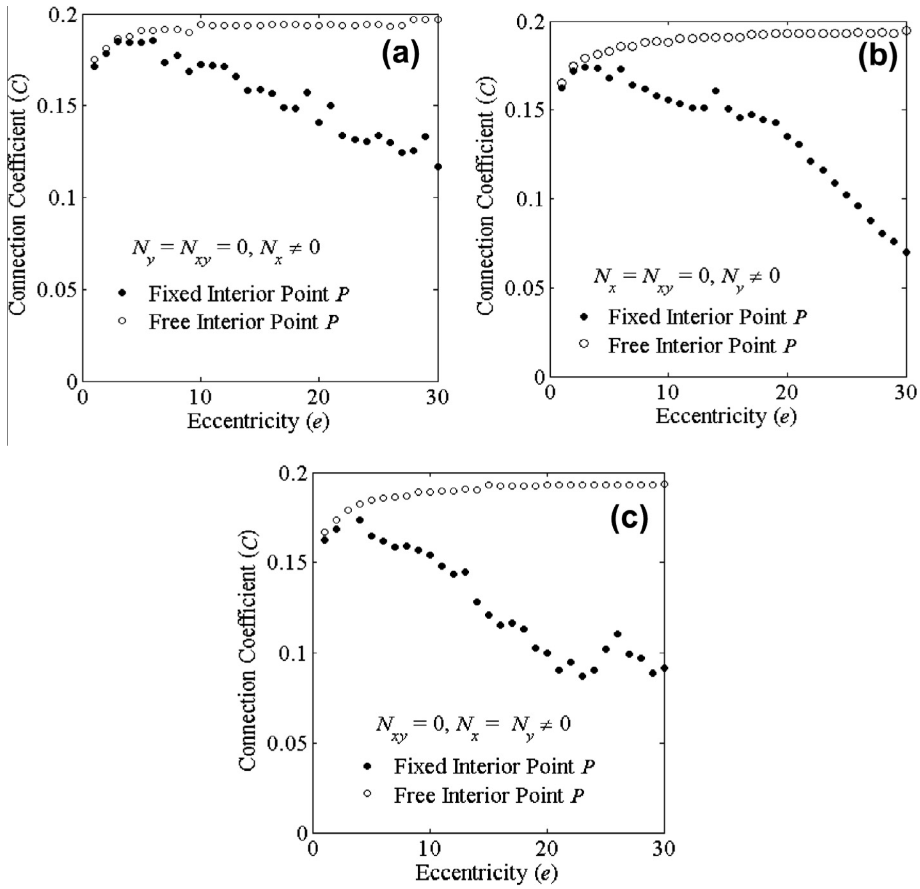

Fig. 5. (a)–(c) Variation of the connection coefficient for load cases (i), (ii) and (iii) respectively, with and without points on the transverse normal through point P clamped. The value of the connection coefficient without clamping any interior point saturates to nearly 0.2 for all loading scenarios. With increasing eccentricity clamping points on the transverse normal through point P divides the region of the plate into two increasingly separated regions in the sense that more modes have negligible amplitude either in region Ω_1 or in region Ω_2.

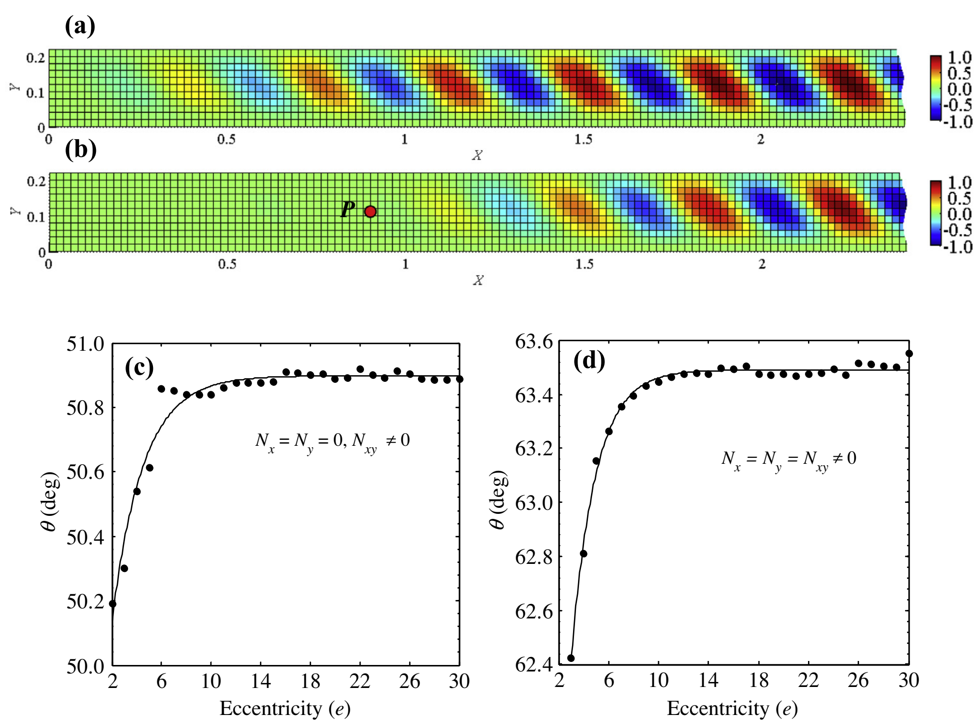

Fig. 6. (a) and (b) top views of the buckling modes of a plate with edge loads $N_x = N_y = 0$, $N_{xy} \neq 0$ and eccentricity = 20 without and with points on a transverse normal through point P clamped, respectively. Contour plot shows the out-of-plane displacement of the plate. The angle θ, shown in Fig. 1, of nodal lines with the horizontal line remains unaffected by clamping of points on the transverse normal through point P. Panels (c) and (d) show variation of the angle θ with the eccentricity for biaxial and combined loads.

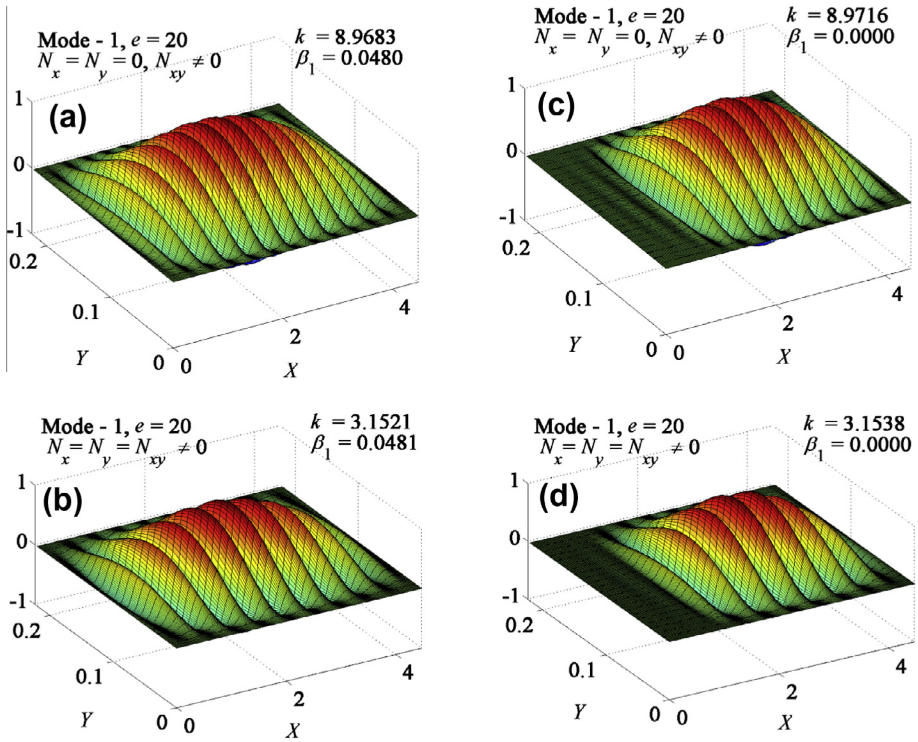

Fig. 7. Normalized 1st buckling mode of a clamped rectangular plate of eccentricity = 20 for different loads on the edges. Modes in figures (a) and (b) are for the cases when only edges of the plate are clamped and those in figures (c) and (d) are for the case when points on the transverse normal through an interior point P are also clamped.

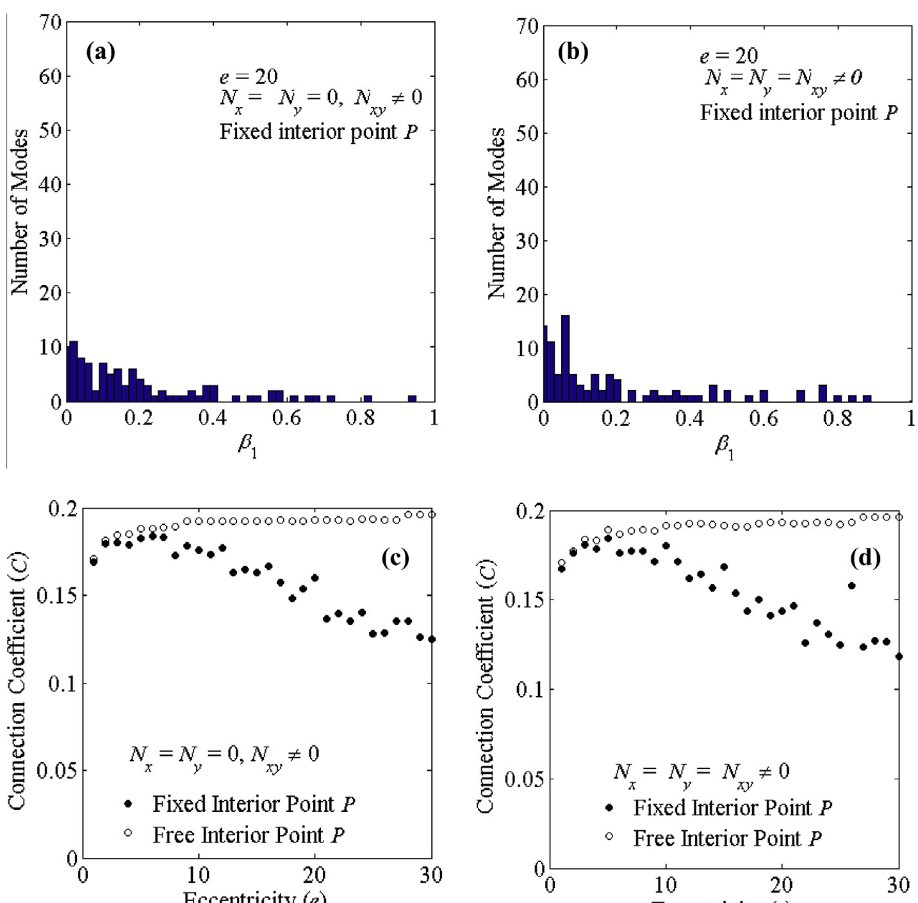

Fig. 8. (a) and (b) distribution of the mode localization parameter β_1 for the loads (iv) and (v). For both types of loads, there is a moderate localization of modes. (c) and (d) variation of the connection coefficient for the load (iv) and (v) with and without clamping points on the transverse normal through point P.

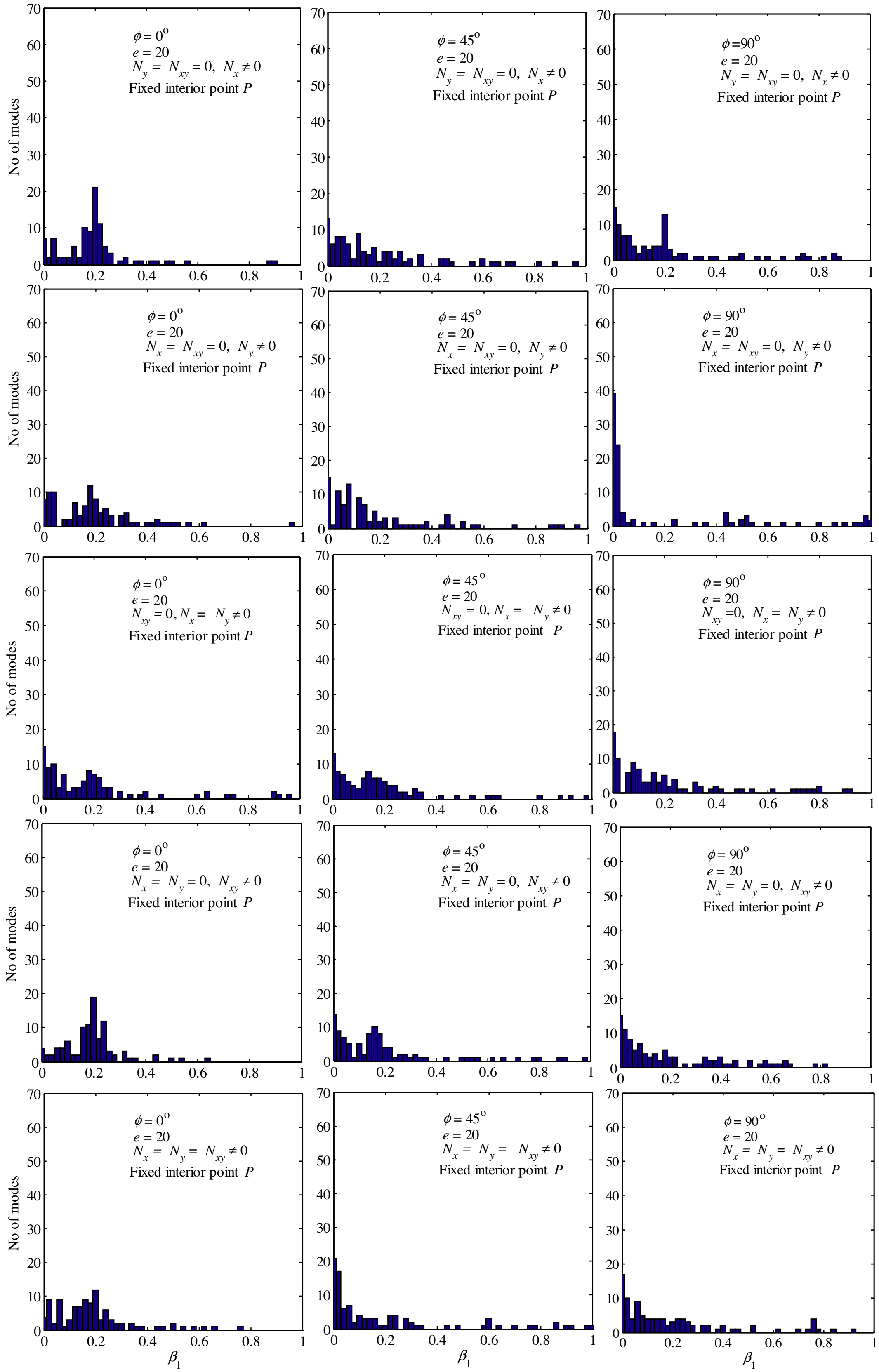

Fig. 9. Distribution of the mode localization parameter β_1 for the five load types for 0°, 45° and 90° laminae. For all these cases the location of point P is shown in Fig. 1.

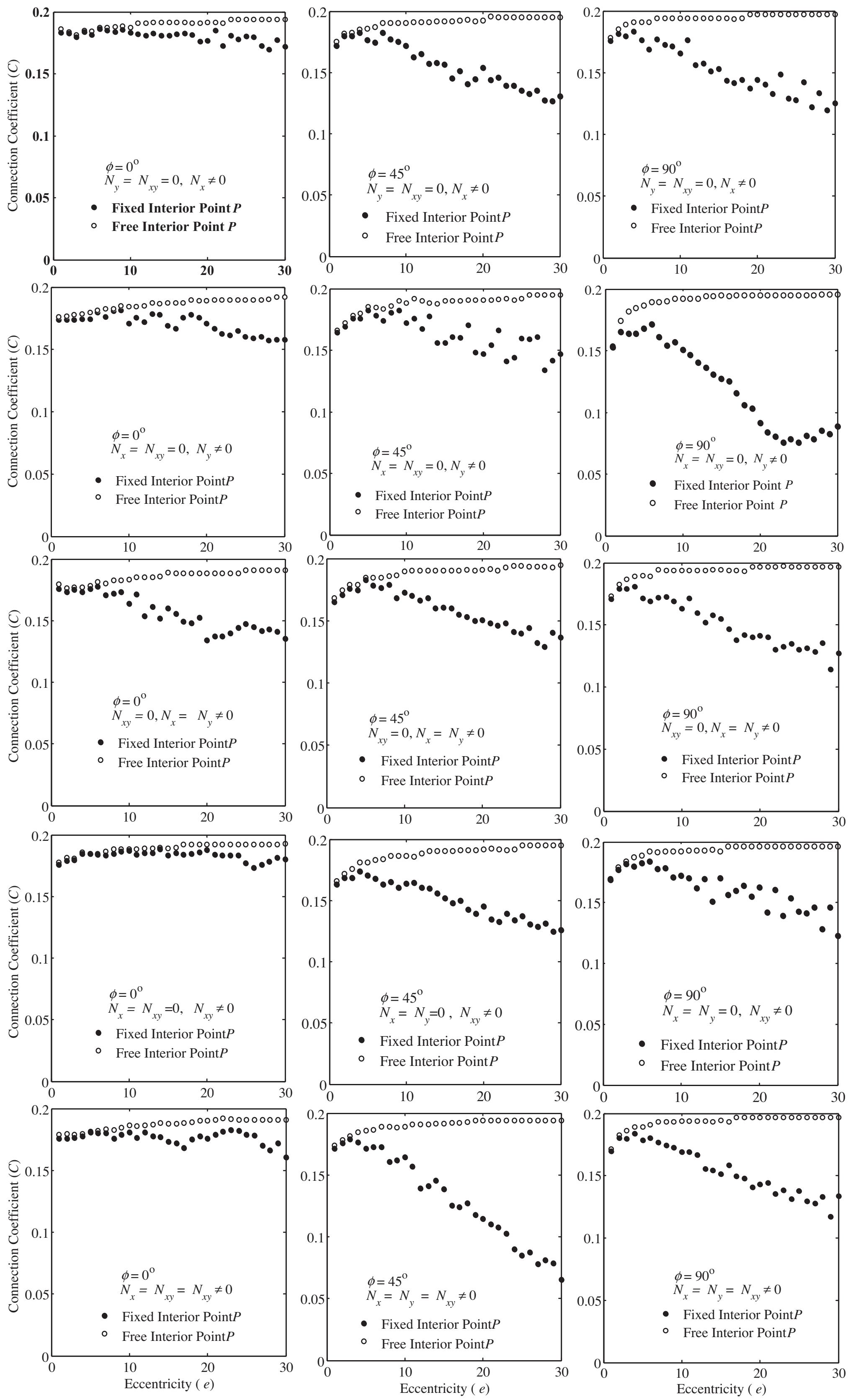

Fig. 10. Variation of the connection coefficient with the eccentricity for the five types of loads for 0°, 45° and 90° laminae. For all these cases the location of point P is shown in Fig. 1.

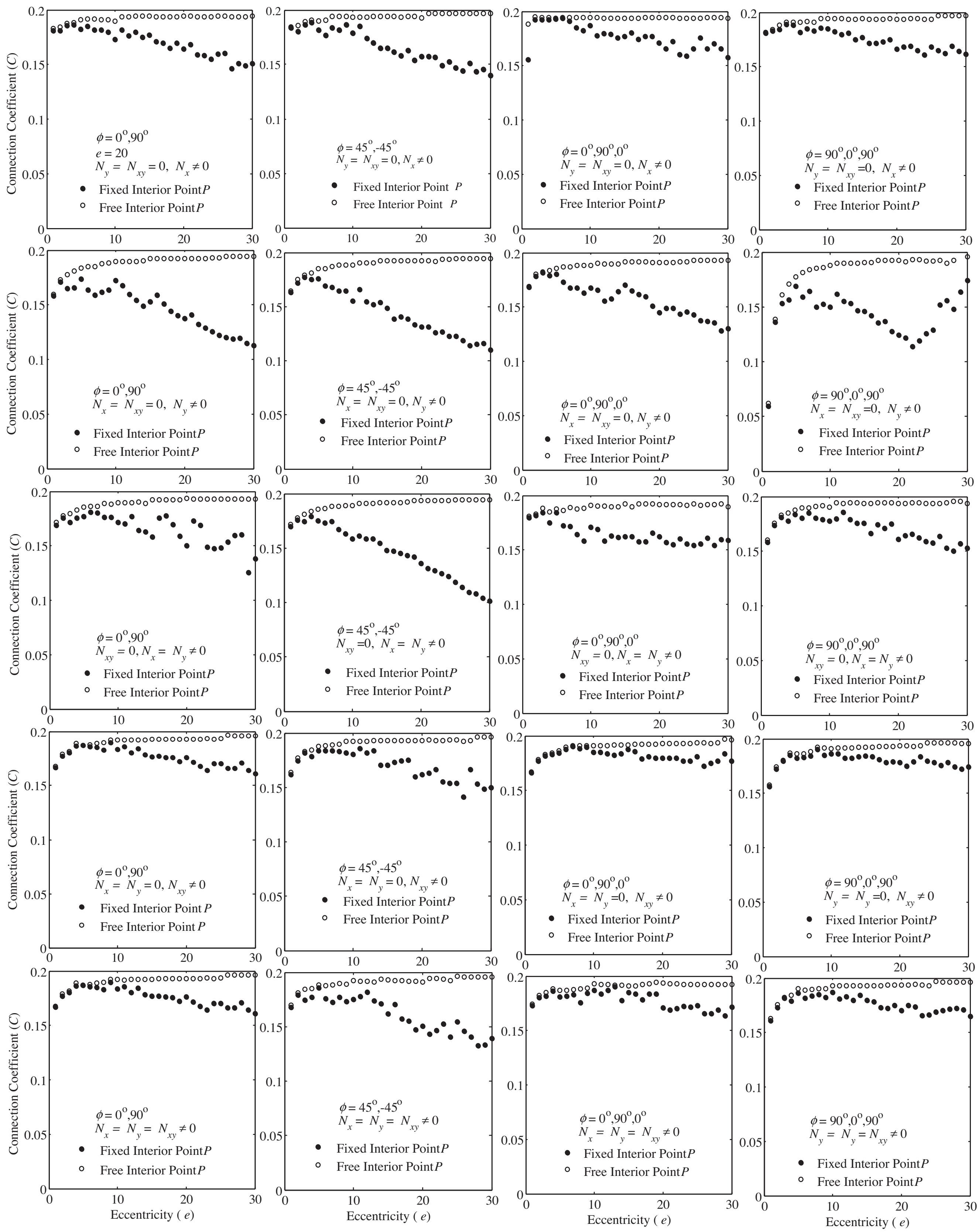

Fig. 11. Variation of the connection coefficient with the eccentricity for the five loading scenarios for antisymmetric 0°/90° and 45°/−45°, and symmetric 0°/90°/0° and 90°/0°/90° laminates. For all these cases the location of point P is shown in Fig. 1.

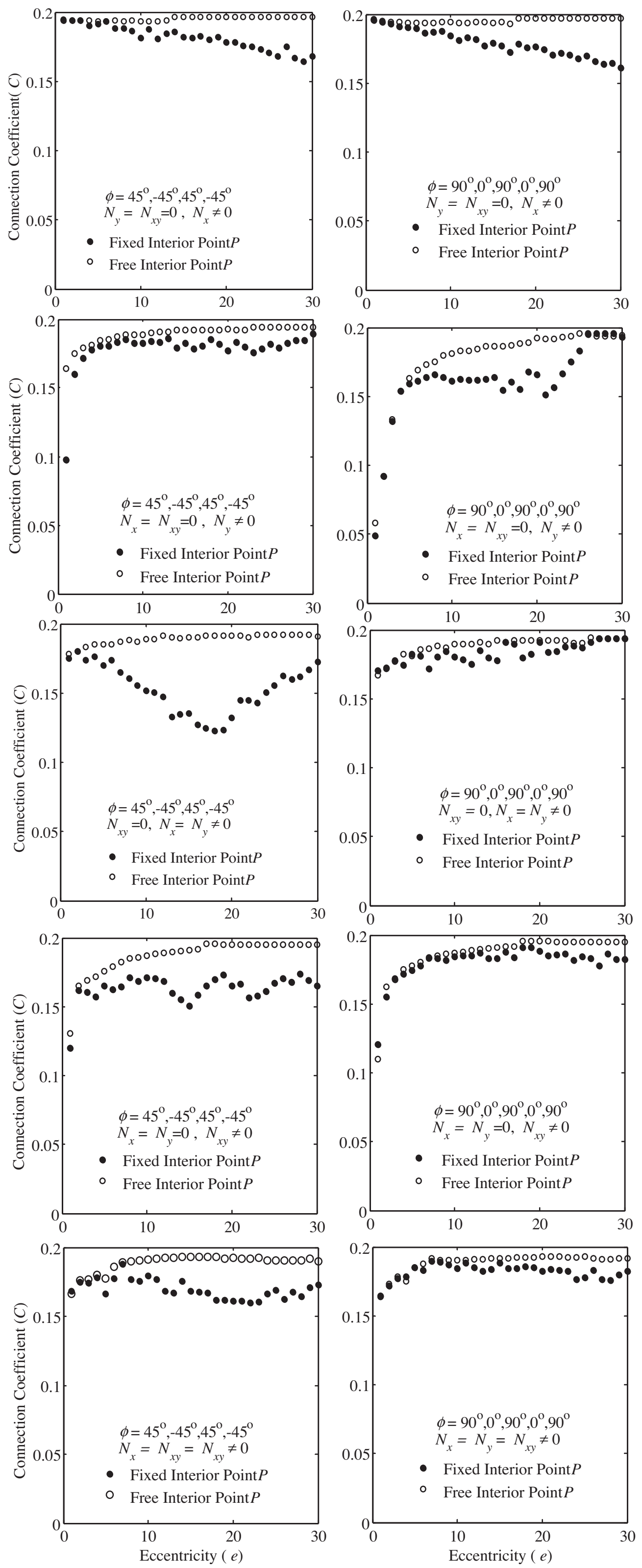

Fig. 12. Variation of the connection coefficient with the eccentricity for the five types of loads for antisymmetric 45°/−45°/45°/−45°, and symmetric 90°/0°/90°/0°/90° laminates. For all these cases the location of point P is shown in Fig. 1.

It is found that for most modes $\beta_1 = 0.2$ which is proportional to the surface area of region Ω_1. However, when the interior point is clamped then the modes get localized as evident from results plotted in Fig. 4b–d. We find that for load (iii) the maximum number of modes get localized in region Ω_2. Furthermore, a low value of β_1 indicates moderate mode localization. Thus, for loads (i) and (ii) there is moderate mode localization.

To quantify dependency of mode localization upon the eccentricity e, we introduce connection coefficient, C, defined [10,11] by

$$C = \frac{1}{S}\sum_{j=1}^{S} \min(\beta_1, (1-\beta_1))_j, \tag{3}$$

where S equals the number of buckling modes of interest. A small value of C implies localization of several buckling modes in either Ω_1 or Ω_2. In Fig. 5 we show variation of C with e for loads (i), (ii) and (iii), and have plotted it for a plate with and without a fixed interior point. For each of the three load types, we find that when the interior point P is not fixed the value of C with an increase in the value of e saturates at 0.2 which is proportional to the surface area of region Ω_1. However, when point P is fixed the value of C decreases with an increase in the value of e. For load (ii) the value of C decreases more rapidly than that for the other two loads.

3.2. Loads (iv) and (v)

The FE simulations reveal that rectangular plates subjected to in-plane either pure shear or combined shear and normal compressive loads with or without an interior clamped point have eigenfunctions with nodal lines inclined at the some angle θ (cf. Fig. 1) to the X-axis, e.g., see Fig. 6a and b for a plate with $e = 20$. Accordingly, the regions of mode localization are trapezoidal rather than rectangular for the plate subjected to in-plane compressive loads only.

In Fig. 7 we have exhibited buckling modes for a plate with the eccentricity $e = 20$ and subjected to loads (iv) and (v) both with and without clamping an interior point. It is found that, for both load types, the clamping of an interior point does not affect the buckling load factor. The buckling load factor is smaller for combined loading as compared to that for the plate subjected to only tangential tractions on the edges. The distribution of mode localization parameter over 100 modes plotted in Fig. 8a and b suggests that the mode localization is weaker than that in the same plate subjected to in-plane compressive loads. However, there are several modes with $0 < \beta_1 < 0.2$ which indicates moderate mode localization. Accordingly, values of the connection coefficient for these loads do not sharply decrease to zero with an increase in the value of e. However, the mode localization increases as evidenced by results exhibited in Fig. 8c and d. Furthermore, with no interior point clamped the connection coefficient stabilizes at 0.2 as for other load types.

3.2.1. Inclination of nodal lines

All nodes with $w(x,y) \sim 0$ are identified and projected on the plane of the plate. Parallel straight lines are fitted through the projected points using the least squares method. The slope of these lines equals the inclination θ of the nodal lines. For $b/h = 100$, values of θ with increasing eccentricity plotted in Fig. 6c and d suggest that θ saturates at 50.89° and 63.55° for loads (iv) and (v), respectively. For thick plates with $b/h = 10$, the saturation values of θ equal 50.06° and 60.61°, respectively. Thus there is no pronounced effect of the plate thickness on the value of θ, however, the nondimensional buckling load is significantly reduced from 8.96 and 3.15 to 6.98 and 2.62 for loads (iv) and (v), respectively. The *critical* buckling load is higher for a thicker plate since it is calculated by multiplying the non-dimensional buckling load by the bending rigidity D.

We note that the inclination angle θ of the line is the same whether or not an interior point P is fixed.

4. Buckling mode localization in orthotropic laminae and laminates

We first investigate mode localization in 0°, 90° and 45° laminae and then in laminates composed of these laminae of uniform thickness, $b/h = 50$, and with material parameters having the following values: $E_1/E_2 = 25$, $G_{12}/E_2 = 0.5$, $G_{23}/E_2 = 0.2$, and $\nu_{12} = 0.25$. The buckling of laminates is analyzed using an equivalent single layer theory.

In Fig. 9 we show the distribution of parameter β_1 over first 100 out-of-plane bending modes for the 0°, 45° and 90° laminae under all five types of loads with a fixed interior point. For each one of the five load types, compared to the 45° and the 90° laminae, the 0° lamina has most modes centered at $\beta_1 = 0.2$ indicating very little mode localization. For the 90° lamina mode localization for load case (ii) is very strong since nearly 40% of the modes are localized in the region Ω_2. In Fig. 10 the degree of mode localization is plotted against the plate eccentricity for the 0°, 45° and 90° laminae. As before for the 0° lamina, the degree of mode localization does not increase with an increase in the plate eccentricity. The degree of mode localization for the 45° and the 90° lamina is found to increase significantly with the increase in the plate eccentricity for load types (v) and (ii), respectively. In general, for the 45° and the 90° laminae the degree of mode localization increases with an increase in the eccentricity.

The variation in the degree of mode localization with the plate eccentricity in two-layered anti-symmetric cross-ply (0°/90°) and angle-ply (45°/−45°) laminates, and in three-layered symmetric cross-ply 0°/90°/0° and 90°/0°/90° laminates for all five load cases is shown in Fig. 11. These results evince that for cross-ply laminates, symmetric or anti-symmetric either there is no appreciable mode localization with increasing aspect ratio or there is no clear trend. For the 45°/−45° laminates subjected to the loads (i), (ii) and (iii) the degree of mode localization is found to increase with an increase in the aspect ratio of laminates. However, the 4-layer angle-ply and the 5-layer cross-ply laminates show only a moderate degree of mode localization as shown in Fig. 12. These results are consistent with those found for the localization of modes of free vibrations in laminates [11] in the sense that localization of modes of vibration in laminates depends upon the localization of modes in individual lamina.

5. Conclusions

By using the Mindlin plate theory and the finite element method with 8-node quadrilateral uniform elements, we have analyzed buckling of clamped–clamped rectangular isotropic plates, orthotropic laminae, and orthotropic laminates with and without fixing points on the transverse normal passing through an interior point for five different in-plane loading conditions. It is found that fixing an interior point divides the plate into two independent regions such that in one of these regions plate's deformations are negligible. For in-plane compressive normal loads on the edges, the two regions are rectangular. However, for in-plane shear or in-plane shear with in-plane normal compressive loads, the two regions are trapezoidal. The inclination of the line passing through the fixed interior point that divides the plate into two regions depends upon the ratio of the plate thickness to the plate width, and the load type. It is found that the localization is pronounced when plates are subjected to in-plane normal compressive loads than that when they are subjected to in-plane shear or in-plane shear and in-plane normal compressive loads. The degree of localization increases with an increase in the aspect ratio of a plate. It is envisaged that fixing an interior point can be used to control buckling failure of plates/laminates.

Acknowledgement

SSG's work was supported by the Office of Naval Research Global Grant No. N62909-14-1-V155 with Dr. Ramesh Kolar as the Associate Director and RCB's work was supported by the Office of Naval Research Grant No. N00014-11-1-0594 with Dr. Y.D.S. Rajapakse as the Program Manager.

References

[1] Hodges CH. Confinement of vibration by structural irregularity. J Sound Vib 1982;82(3):411–24.
[2] Pierre C, Dowell EH. Localization of vibrations by structural irregularity. J Sound Vib 1987;114(3):549–64.
[3] Pierre C, Plaut RH. Curve veering and mode localization in a buckling problem. J Appl Math Phys 1989;40:758–61.
[4] Nayfeh AH, Hawwa MA. Use of mode localization in passive control of structural buckling. AIAA J 1994;32(10):2131–3.
[5] Li YW, Elishakoff I, Starnes Jr JH. Buckling mode localization in multi-span periodic structure with a disorder in a single span. Chaos Solitons Fractals 1995;5(6):955–69.
[6] Elishakoff I, Li YW, Starnes Jr JH. Buckling mode localization in elastic plates due to misplacement in stiffener location. Chaos Solitons Fractals 1995;5(8):1517–31.
[7] Xie W-C, Ibrahim A. Buckling mode localization in rib-stiffened plates with misplaced stiffeners – a finite strip approach. Chaos Solitons Fractals 2000;11(10):1543–58.
[8] Xie W-C. Buckling mode localization in nonhomogeneous beams on elastic foundations. Chaos Solitons Fractals 1997;8(3):411–31.
[9] Brasil RM, Hawwa MA. The localization of buckling modes in nearly periodic trusses. Comput Struct 1995;56(6):927–32.
[10] Filoche M, Mayboroda S. Strong localization induced by clamped point in thin plate vibration. Phys Rev Lett 2009;103:254301.
[11] Sharma D, Gupta SS, Batra RC. Mode localization in composite laminates. Compos Struct 2012;94:2620–31.
[12] Verma D, Gupta SS, Batra RC. Vibration mode localization in single- and multi-layered graphene nanoribbons. Comp Mater Sci 2014;95:41–52.
[13] User's manual 2005, MATLAB. The Math Works Inc., MA, USA.
[14] Timoshenko [14]S, Gere M. Theory of elastic stability. McGraw Hill International Book Company; 1985.
[15] Shufrin I, Eisenberger M. Shear buckling of thin plates with constant in-plane stresses. Int J Struct Stab Dyn 2007;7(2):179–92.
[16] Shufrin I, Rabinovitch O, Eisenberger M. Buckling of symmetrically laminated rectangular plates with general boundary conditions – A semi analytical approach. Compos Struct 2008;82(4):521–31.